Molecular Crystals and Liquid Crystals
Publication details, including instructions for authors and subscription information:
http://www.tandfonline.com/loi/gmcl16

Measurements of Hydrodynamic Parameters for Nematic 5CB

K. Skarp [a] , S. T. Lagerwall [a] & B. Stebler [a]
[a] Physics Department,, Chalmers University of Technology, S-412 96, Göteborg, Sweden
Version of record first published: 20 Apr 2011.

To cite this article: K. Skarp , S. T. Lagerwall & B. Stebler (1980): Measurements of Hydrodynamic Parameters for Nematic 5CB, Molecular Crystals and Liquid Crystals, 60:3, 215-236

To link to this article: http://dx.doi.org/10.1080/00268948008072401

Mol. Cryst. Liq. Cryst., 1980, Vol. 60, pp. 215–236
0026-8941/80/6003–0215$04.50/0

Measurements of Hydrodynamic Parameters for Nematic 5CB.

K. SKARP, S. T. LAGERWALL and B. STEBLER

Physics Department, Chalmers University of Technology, S-412 96 Göteborg, Sweden

(*Received October 31, 1979*)

A nematic liquid crystal, pentyl-cyano-biphenyl (5CB) is studied in two different flow situations: Poiseuille flow and torsional shear flow, in both cases with and without the simultaneous application of an electric field. The Poiseuille flow set-up gives an accurate determination of the Miesowicz viscosity η_c and a less precise estimation of η_b. With η_c known it is possible to separately determine the elastic constants K_{11} and K_{33} and the viscous coefficients α_2, α_3, and thereby γ_1, γ_2, from the torsional shear flow experiment. Using the data we have also been able to calculate the actual director profile in the liquid crystal as a function of applied shear and electric field. Curves are given of K_{11}, K_{33}, K_{11}/K_{33}, α_2, α_3, γ_1, γ_2, γ_1/γ_2, η_b and η_c for 5CB as a function of temperature through the whole nematic range from 22.0 °C to 35.1 °C.

I INTRODUCTION

The hydrodynamics of anisotropic liquids is considerably different from that of ordinary liquids. For nematics, the simplest class of liquid crystals, a continuum description has been worked out by Ericksen and Leslie,[1] in which the liquid is characterized by five independent viscosity parameters and three curvature elasticity parameters. The viscosities are the so called Leslie friction coefficients α_i, $i = 1, \ldots, 6$, one of which can be expressed in the others by an Onsager relation.[2] The elasticities are the Oseen–Zocher–Frank (OZF) constants K_{ii}, $i = 1, 2, 3$ for splay, twist and bend respectively, which also determines the static behaviour of the liquid crystal. For a complete macroscopic description the knowledge of all the α_i's and K_{ii}'s as a function of temperature would be required; in practice this has rarely been achieved, especially regarding the α_i's. Fortunately, not all of them are of equal importance.

To describe the flow of a nematic two fields have to be specified in the medium: the velocity $\mathbf{v}(\mathbf{r}, t)$ and the director $\hat{\mathbf{n}}(\mathbf{r}, t)$. The boundary

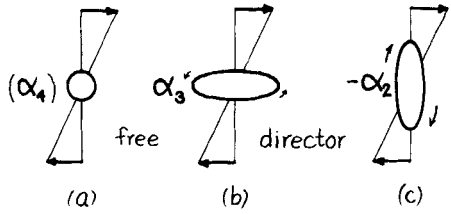

FIGURE 1 Physical meaning of Leslie viscosities α can be related to the director behaviour in a simple shear. Only two of $\alpha_4, \alpha_3, \alpha_2$ correspond to director torques (α_2, α_3). In (a) α_4 only symbolizes a viscosity characteristic for the local director alignment, which is furthermore unstable above a certain shear threshold.[19]

conditions of both variables are important. The unit vector $\hat{\mathbf{n}}$ is degenerate in sign, is not linked to any conservation law and can hardly be unambiguously defined, nevertheless it is indispensable in the description. It describes the direction in space of the local anisotropy ("average local molecular orientation") and has to be referred to some convenient macroscopic tensor property for its measurement, like the refractive index. We will assume it to be equivalent to the local optic axes in the medium. Experimentally this means that we will map the director field in a steady state flow situation by using optical techniques.

A central point in the Ericksen-Leslie description is the coupling between $\mathbf{v}$ and $\hat{\mathbf{n}}$. A velocity gradient $\nabla\mathbf{v}$ exerts a viscous torque on the director, and, conversely, a local rotation of the director may induce a flow. To appreciate the meaning and importance of the different viscosities we may look at the torque on the director in a simple linear shear flow, illustrated in Figures 1 and 2. Three extreme initial director alignments are shown. The first corresponds to no torque, and is less interesting in this connection. The parameter α_4 corresponds to a director independent stress term and thus appears like the viscosity for an ordinary liquid. The second situation gives a (normally weak) torque determined by α_3 in sign and magnitude (anti-clockwise if

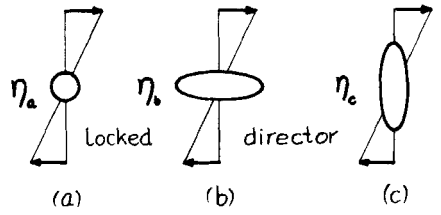

FIGURE 2 Physical meaning of Miesowicz viscosities $\eta_{a,b,c}$ relate to a flow where the director is locked in direction. The η's are effective viscosities characteristic for resistance and dissipation in the three situations shown. The viscosities ($\eta_b < \eta_a < \eta_c$) can be expressed as $\eta_a = 1/2\alpha_4$, $\eta_b = 1/2(\alpha_3 + \alpha_4 + \alpha_6)$, $\eta_c = 1/2(-\alpha_2 + \alpha_4 + \alpha_5)$.

$\alpha_3 < 0$), the third a strong clockwise torque determined by α_2, which means that α_2 is always negative.

Of the five independent α's, α_2 and α_3 are the most important hydrodynamic parameters. Their relative sign and magnitude will determine the response of the director to a shear. If we write $\gamma_1 \equiv \alpha_3 - \alpha_2$ and $\gamma^3 \equiv \alpha_3 + \alpha_2$ then γ_1 measures the torque density from the rotational part of the velocity field, whereas γ_2 similarly characterizes the irrotational part. From the ratio $|\gamma_1/\gamma_2|$ we either obtain information of the equilibrium alignment angle θ_0 between the director and the local velocity in a shear (if <1), or the information that there is no stable alignment angle at all (if >1).

The quantity $\gamma_1(\gamma_1 > 0)$ in itself determines the relaxation behaviour of the director. Its name, twist viscosity, is appropriate for several reasons. Of the effective nematic viscosities measured by light scattering it shows to be identical to the twist viscosity η_T, whereas it appears in the splay and bend viscosities η_S and η_B in combination with two other important viscosities η_b and η_c ($\eta_S = \gamma_1 - \alpha_3^2/\eta_b$, $\eta_T = \gamma_1$, $\eta_B = \gamma_1 - \alpha_2^2/\eta_c$). The so called Miesowicz viscosities η_a, η_b and η_c are defined in Figure 2. The difference from the situation in Figure 1 is that the flow occurs with the director locked in space and time to one of the situations (*a*), (*b*), (*c*), usually by using a strong external electric or magnetic field.

The measurements of this reported work give, apart from K_{11} and K_{33}, the values of α_2, α_3, η_b, η_c and thereby combinations like γ_1, γ_2, η_S, η_T and η_B as a function of temperature. The rotational shear flow method was pioneered by Wahl and Fischer[3] and by Waltermann and Fischer[4] who also considered the effect of a magnetic field on the nematic flow. They obtained in this way the ratios K_{33}/K_{11}, γ_2/γ_1 and K_{33}/χ_a. Holmström and Lagerwall[5] proposed to use an electric field together with the shear in order to split the ratios and determine the elastic constants and viscosities separately. However, as discussed in detail in section IIIb, the split relies on a two-parameter fit to a parabolic curve, whose deviation from linearity shows to be very weak in practice, thereby making the determination too imprecise. The determination therefore requires the combination of two different shear geometries as used in this work.

There exist in the literature different conventions for the signs of γ_1 and γ_2. In Leslie's original treatment,[6] where γ_1 is defined as $\gamma_1 = \alpha_2 - \alpha_3$, it is shown by thermodynamic inequalities that $\gamma_1 \leq 0$. This sign convention is used in Refs. 1, 3, 6, 7, but has some practical disadvantages. The opposite sign convention is used by de Gennes,[8] Stephen and Straley[9] and in practically all papers on technical applications of liquid crystals. It is true that the sign convention is just a matter of choice. On the other hand, in all applied work, γ_1 characterizes relaxation processes, and a negative γ_1 would appear in a most unnatural way, giving seemingly growing instead of decaying

exponential factors. For this reason we will adhere to the sign convention of Refs. 8, 9, i.e. our Eq. (13) and the constraint $\gamma_1 \geq 0$. This means that we have changed sign convention relative to Ref. 5, which has necessitated a considerable rewriting and re-shaping of basic equations. We also take advantage of the reformulation to alter and simplify some of the notation and to correct some inconsistencies in Ref. 5. The expressions (56) and onwards of Ref. 5 are based on an approximation requiring ε small, which turns out to be violated even at quite weak electric fields and also leads to a wrong field dependence for the alignment in Eq. (64) of that work. The relations (38) to (46) of this paper are the corresponding correct expressions involving a higher order approximation in solving Eq. (35).

Nematics are the, to date, most technologically important liquid crystals. It might be appropriate in closing this section to mention that of the different viscosities γ_1 is the most important technical parameter for the response times of display cells. Of the elastic constants K_{11} has a dominating influence on the switching threshold, whereas the ratio K_{11}/K_{33} has a decisive influence on the sharpness of this threshold (sharper the higher this value) and thus on multiplexing properties.

II SIMPLE SHEAR FLOW: THEORY

a Derivation of the basic equations

Starting from the Ericksen–Leslie equations we specialize the problem to describe a simple shear flow in an electric field, and obtain two coupled differential equations for the director and the velocity gradient. We then make an ansatz for the director valid for low shear rates and weak electric fields. With this ansatz we obtain an analytical solution of the director equation in terms of elasticity and viscosity constants subsequently used in section III for the experimental evaluation of the material parameters.

The conservation laws are, in the Cartesian tensor notation with the usual summation convention,

$$\rho \dot{v}_j = f_j + \sigma_{ij,i} \tag{1}$$

$$I \dot{n}_j = g_j + \pi_{ij,i} \tag{2}$$

A superposed dot denotes a material time derivative. Equation (1) is the conservation of linear momentum, the constant ρ being the density, f_i any external body force acting, except electromagnetic forces, which we choose to include in the stress tensor σ_{ij} through the Maxwell stress tensor σ_{ij}^{em}. The only contribution to f_i in our problem comes from gravitational forces, which we do not take into account; we thus set $f_i = 0$. Equation (2) is

equivalent to the conservation of angular momentum, I being the moment of inertia density, g_i the intrinsic director torque density and π_{ij} the director surface stress. The inertial term in this equation will be dropped as it only comes into play at very high frequencies. The use of Eqs. (1) and (2) requires constitutive assumptions on torques and stresses. The elastic energy is a quadratic function in the director gradients and is given by the Oseen–Frank expression. If we include the electromagnetic contribution, the free energy can be written

$$F = \tfrac{1}{2}\{K_{11}(n_{i,i})^2 + K_{22}(\varepsilon_{ijk}\, n_i n_{k,j})^2 + K_{33} n_i n_j n_{k,i} n_{k,j} - D_i E_i - B_i H_i\} \tag{3}$$

The elastic and electromagnetic part of the stress tensor can then be written

$$\sigma^0_{ij} = -\frac{(\partial F/\partial n_{k,j})}{n_{k,i}} \tag{4}$$

$$\sigma^{em}_{ij} = \tfrac{1}{2}\{D_i E_j + D_j E_i + B_i H_j + B_j H_i - (D_k E_k + B_k H_k)\delta_{ij}\} \tag{5}$$

If we then denote the viscous part of σ_{ij} by $\hat{\sigma}_{ij}$, the expressions for torques and stresses assume the form

$$g_i = n_i \lambda - (n_i \beta_j)_{,j} - \frac{\partial F}{\partial n_i} - \tilde{g}_i \tag{6}$$

$$\pi_{ij} = n_i \beta_j + \frac{\partial F}{\partial n_{i,j}} \tag{7}$$

$$\sigma_{ij} = -p\delta_{ij} + \sigma^0_{ij} + \hat{\sigma}_{ij} + \sigma^{em}_{ij} \tag{8}$$

In Eq. (8) the scalar p is the usual arbitrary pressure arising from the incompressibility assumption. In a similar way, the scalar λ and the vector β_i (which may be treated as Lagrange multipliers) represent indeterminacies due to the constraint on the variable $\hat{n}$.

The most important constitutive assumptions concern the intrinsic director body force $\tilde{g}_i$ and the viscous stress $\hat{\sigma}_{ij}$ (the hydrodynamic part of the stress). Both are taken to be linear functions of the director n_i, of the angular velocity of the director relative to that of the fluid, N_i,

$$N_i = \dot{n}_i + \tfrac{1}{2}(v_{j,i} - v_{i,j})n_j \tag{9}$$

and of the symmetric part of the velocity gradient, A_{ij},

$$A_{ij} = \tfrac{1}{2}(v_{i,j} + v_{j,i}) \tag{10}$$

General arguments, going back to Leslie,[6] show that

$$\tilde{g}_i = \gamma_1 N_i + \gamma_2 A_{ik} n_k \tag{11}$$

where γ_1 and γ_2 are viscosities related to the α's (see below), and further, that

$$\hat{\sigma}_{ij} = \alpha_1 n_k n_p A_{kp} n_i n_j + \alpha_2 N_i n_j + \alpha_3 N_j n_i + \alpha_4 A_{ij} + \alpha_5 A_{ik} n_k n_j + \alpha_6 A_{jk} n_k n_i \quad (12)$$

Between α's and γ's the following relations are valid

$$\gamma_1 = \alpha_3 - \alpha_2, \gamma_2 = \alpha_6 - \alpha_5 = \alpha_3 + \alpha_2 \quad (13)$$

the very last equality being known as the Onsager–Parodi relation.

Finally, we will in this section make use of the following relations for electric and magnetic fields in an anisotropic medium

$$D_i = (\varepsilon_\perp \delta_{ij} + \varepsilon_a n_i n_j) E_j, \; B_i = (\mu_\perp \delta_{ij} + \mu_a n_i n_j) H_j \quad (14)$$

where ε_a and μ_a are the anisotropies in the susceptibilities, $\varepsilon_a = \varepsilon_\parallel - \varepsilon_\perp$ and $\mu_a = \mu_\parallel - \mu_\perp$ ($\perp$denotes perpendicular and $\parallel$ parallel to the director).

b Application to the present problem

In the experiment a torsional shear is used, where the liquid crystal is held between two circular glass plates, one of them rotating with a low angular velocity. In this geometry we in principle have a radial and a vertical velocity gradient, but as the radii at which the flow is observed are much larger than the thickness of the liquid crystal layer, the radial velocity gradient can be neglected. Consequently, we can well approximate the circular motion locally with a linear motion.

When a shear is applied in the x-direction (see Figure 3), the director will tilt from the z-axis. A simultaneously applied electric field will also influence the director and the local shear rate. Experimentally, we observe the development of a stationary director configuration after a certain relaxation time (usually a few minutes). For the stationary state we set $\dot{n}_i = 0$ and

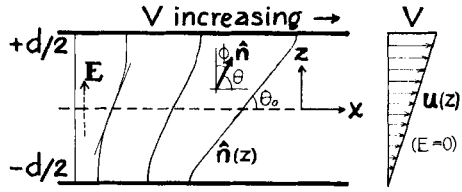

FIGURE 3 Geometry of the shear flow problem. The point $z = 0$ is half-way between the plates. The distance between the plates is d. E is the applied electric field, and V the local shear velocity $V = \omega R$. Solutions to the flow problem are discussed for the director $\hat{\mathbf{n}}$ lying in the x–z plane and making an angle ϕ to the z-axis. The equilibrium value of the complement angle θ, θ_0, in a shear flow is usually called the flow alignment angle.

$\dot{v}_i = 0$ in the continuum equations. Further, we restrict the director to lie in the x–z plane, and set $n_y = 0$. With these assumptions and the constraints $v_{i,i} = 0$ (arising from incompressibility) and $n_i n_i = 1$, we are lead to investigate solutions of the form

$$n_x = \sin\phi, \qquad n_y = 0, \qquad n_z = \cos\phi, \qquad \phi = \phi(z)$$
$$v_x = u(z), \qquad v_y = 0, \qquad v_z = 0 \tag{15}$$

To avoid electrohydrodynamic instabilities we use an a.c. electric field. We can treat the liquid crystal as a dielectric, ignoring conductivity, and write the sinewave field applied to the sample as $\mathbf{E} = (0, 0, E)$, where E is the rms-value, $E = E_0/\sqrt{2}$, E_0 being the amplitude.

We now insert the expressions (15) defining the present problem into the balance laws Eqs. (1) and (2) and get four equations

$$(\hat{\sigma}_{zx} + \sigma^{em}_{zx})_{,z} = 0 \tag{16}$$

$$(-p + \sigma^0_{zz} + \hat{\sigma}_{zz} + \sigma^{em}_{zz})_{,z} = 0 \tag{17}$$

$$\lambda n_x - \tilde{g}_x + \pi_{zx,z} = 0 \tag{18}$$

$$\lambda n_z - \partial F/\partial n_z - \tilde{g}_z + \pi_{zz,z} = 0 \tag{19}$$

Equation (17) determines the pressure p which is of no concern here, and this equation will not be considered any further. We eliminate the scalar λ between Eqs. (18) and (19), and the resulting equation, together with Eq. (16) will be the relevant equations for our shear flow. Into these two equations we insert the constitutive expressions (3)–(14), evaluated with Eq. (15).

After rather lengthy but straightforward calculations (cf. Ref. 5) we arrive at two coupled non-linear differential equations for $\phi(z)$ and $u(z)$:

$$2f(\phi)\frac{\mathrm{d}^2\phi}{\mathrm{d}z^2} + \frac{\mathrm{d}f}{\mathrm{d}\phi}\left(\frac{\mathrm{d}\phi}{\mathrm{d}z}\right)^2 + \frac{1}{2}\frac{\mathrm{d}u}{\mathrm{d}z}(\gamma_1 - \gamma_2\cos 2\phi) - \varepsilon_a E^2 \cos\phi \sin\phi = 0 \tag{20}$$

$$\frac{\mathrm{d}}{\mathrm{d}z}\left(g(\phi)\frac{\mathrm{d}u}{\mathrm{d}z} + \frac{1}{2}\varepsilon_a E^2 \cos\phi \sin\phi\right) = 0 \tag{21}$$

where we have introduced the expressions

$$f(\phi) = K_{11}\sin^2\phi + K_{33}\cos^2\phi \tag{22}$$

and

$$2g(\phi) = 2\alpha_1 \sin^2\phi\cos^2\phi + (\alpha_5 - \alpha_2)\cos^2\phi + (\alpha_3 + \alpha_6)\sin^2\phi + \alpha_4 \tag{23}$$

If we introduce the Miesowicz viscosities η_b and η_c defined by $2\eta_b = \alpha_3 + \alpha_4 + \alpha_6$ and $2\eta_c = \alpha_4 + \alpha_5 - \alpha_2$, we can write

$$g(\phi) = \eta_b \sin^2\phi + \eta_c \cos^2\phi + \alpha_1 \cos^2\phi \sin^2\phi \tag{24}$$

Eq. (21) may be integrated at once to give

$$g(\phi)\frac{du}{dz} + \frac{1}{2}\varepsilon_a E^2 \sin\phi\cos\phi = a \tag{25}$$

where a is an integration constant giving the shear force per unit area applied to the moving plate.

We now substitute du/dz given in Eq. (25) into Eq. (20), simultaneously introducing the expression $\cos 2\phi_0 = \gamma_1/\gamma_2$, where ϕ_0 is the complement to the flow alignment angle θ_0, and changing to a dimensionless coordinate defined by $\zeta = 2z/d$, d being the liquid crystal layer thickness. Equations (20) and (21) then become

$$2f(\phi)\frac{d^2\phi}{d\zeta^2} + \frac{df}{d\phi}\left(\frac{d\phi}{d\zeta}\right)^2 - \frac{\cos 2\phi - \cos 2\phi_0}{g(\phi)}\gamma_2(a_0 - \kappa_0\cos\phi\sin\phi) - 4\kappa_0\cos\phi\sin\phi = 0 \tag{26}$$

$$\frac{du}{d\zeta} = \frac{2}{d}\frac{a_0 - \kappa_0\cos\phi\sin\phi}{g(\phi)} \tag{27}$$

The quantities a_0 and κ_0 are given by $a_0 = ad^2/4$ and $\kappa_0 = \varepsilon_a E^2 d^2/8 = \varepsilon_a U^2/8$, where U is the rms-value of the applied voltage.

A full description of the flow is contained in Eqs. (26) and (27) supplemented with the boundary conditions $\phi(\pm 1) = 0$, $u(-1) = 0$, $u(1) = V$. The complexity of these equations makes it impossible to find any useful general solution. However, it turns out that a lot of information can be obtained about the nematic by studying it under very low shears and weak electric fields. This means that the director angle $\phi(\zeta)$ will always be a small angle, pointing on the possibility of making a simple ansatz for $\phi(\zeta)$ and inserting it into Eqs. (26) and (27) to evaluate the constants in the ansatz in terms of material coefficients and external actions (V and E).

c Solution for a weakly distorted director [$\phi(\zeta)$ small]

The influence of the shear and the electric field on the nematic is studied optically, through the change in the effective birefringence. Let $n_e(\phi)$ denote the extraordinary and n_0 the ordinary refractive index [$n_e(\phi) \geq n_0$]. The mean optical anisotropy across the liquid crystal layer is then given by

$$\langle n_e(\phi) - n_0\rangle = \int_0^1 [n_e(\phi) - n_0]d\zeta \tag{28}$$

with

$$n_e(\phi) - n_0 = n_\perp\{[1 - (1 - n_\perp^2/n_\parallel^2)\sin^2\phi]^{-1/2} - 1\} \tag{29}$$

where $n_{\|}$ is the extremal refractive index and $n_{\perp} = n_0$. For small ϕ this can be expanded to give

$$n_e(\phi) - n_o = \tfrac{1}{2}n_{\perp}\left(1 - \frac{n_{\perp}^2}{n_{\|}^2}\right)(\phi^2 - \tfrac{1}{3}\phi^4 + \cdots) \tag{30}$$

We make the same ansatz for $\phi(\zeta)$ as in Refs. (3) and (5)

$$\phi(\zeta) = \Phi(1 - \zeta^2)(1 + \varepsilon\zeta^2) \tag{31}$$

motivated by the fact that it approximates extremely well the exact solution of the linearized form of Eq. (26). Φ is the maximum value of ϕ attained in the middle of the layer. If we insert Eq. (31) into Eq. (30) and integrate according to Eq. (28), we get, to first order in ε

$$\langle n_e - n_o\rangle = \tfrac{1}{2}n_{\perp}\left(1 - \frac{n_{\perp}^2}{n_{\|}^2}\right)\{\tfrac{8}{15}\Phi^2(1 + \tfrac{2}{7}\varepsilon) - \tfrac{128}{945}\Phi^4(1 + \tfrac{4}{11}\varepsilon)\} \tag{32}$$

We observe the nematic film subjected to a torsional shear in parallel monochromatic light between crossed polarizers. The light is incident normal to the film. Because the shear induced effective birefringence along the light path increases with the shear rate, which increases radially outwards, the optical pattern seen consists of concentric dark rings, cf. Figure 5. The extinction condition for dark rings is

$$\frac{m}{d} = \frac{\langle n_e - n_o\rangle}{\lambda_0} \tag{33}$$

where m is the ring number, beginning with $m = 0$ at the center, and λ_0 is the wavelength of the incident light. Since $\langle n_e - n_o\rangle$ is what we observe experimentally, we want to replace the parameters Φ and ε on the right-hand side of Eq. (32) with the material coefficients for the nematic and the shear velocity and the applied electric field, $\Phi = \Phi(K_{ii}, \alpha_i, V, E)$ and $\varepsilon = \varepsilon(K_{ii}, \alpha_i, V, E)$. We get these expressions for Φ and ε by inserting Eq. (31) into Eqs. (26) and (27) expanded into zeroth and first order in $\phi(\zeta)$, and identifying terms.

Series expansion to first order in ϕ gives

$$\left.\begin{aligned} &f(\phi) = K_{33},\ \frac{df}{d\phi} = 2\phi(K_{11} - K_{33}),\ \frac{d^2\phi}{d\zeta^2} = 2\Phi\left(-1 - 5\varepsilon + 6\varepsilon\frac{\phi}{\Phi}\right),\\ &\left(\frac{d\phi}{d\zeta}\right)^2 = 4\Phi^2\left((1 + \varepsilon)^2 - (1 + 5\varepsilon)\frac{\phi}{\Phi}\right),\ 4\kappa_0\cos\phi\sin\phi = 4\kappa_0\phi,\\ &\frac{\cos 2\phi - \cos 2\phi_0}{g(\phi)}\gamma_2(a_0 - \kappa_0\cos\phi\sin\phi)\\ &\quad = \frac{\kappa_0(\gamma_1 - \gamma_2)}{\eta_c}\phi - \frac{a_0(\gamma_1 - \gamma_2)}{\eta_c} \end{aligned}\right\} \tag{34}$$

Insertion into Eqs. (26) and (27) yields

$$\left.\begin{aligned} &-4K_{33}\Phi - 20K_{33}\Phi\varepsilon + 24K_{33}\varepsilon\phi + 8K_{11}\Phi^2(1+\varepsilon)^2\phi \\ &-8K_{33}\Phi^2(1+\varepsilon)^2\phi - \frac{\kappa_0(\gamma_1-\gamma_2)}{\eta_c}\phi + \frac{a_0(\gamma_1-\gamma_2)}{\eta_c} - 4\kappa_0\phi = 0 \\ &\frac{\mathrm{d}u}{\mathrm{d}\zeta} = \frac{2}{\mathrm{d}}\left(\frac{a_0}{\eta_c} - \frac{\kappa_0}{\eta_c}\phi\right) \end{aligned}\right\} \tag{35}$$

The velocity gradient is integrated

$$\int_0^V \mathrm{d}u = \frac{2}{\mathrm{d}}\int_{-1}^{1}\left\{\frac{a_0}{\eta_c} - \frac{\kappa_0}{\eta_c}\Phi(1-\zeta^2)(1+\varepsilon\zeta^2)\right\}\mathrm{d}\zeta \tag{36}$$

with the result, slightly rearranged

$$\frac{a_0}{\eta_c} = \frac{V\mathrm{d}}{4} + \frac{2}{3}\frac{\kappa_0}{\eta_c} \tag{37}$$

The zeroth order terms in the director equation give

$$\Phi(1+5\varepsilon) - \frac{a_0(\gamma_1-\gamma_2)}{4K_{33}\eta_c} = 0 \tag{38}$$

The first order terms give, solved for ε

$$\varepsilon = \frac{\kappa_0}{24K_{33}}\left(4 + \frac{\gamma_1-\gamma_2}{\eta_c}\right) + \left[1 + \frac{\kappa_0}{12K_{33}}\left(4 + \frac{\gamma_1-\gamma_2}{\eta_c}\right) + \frac{\kappa_0^2}{576K_{33}^2}\left(4 + \frac{\gamma_1-\gamma_2}{\eta_c}\right)^2\right]\frac{K}{3}\Phi^2 \tag{39}$$

where $K = (K_{33} - K_{11})/K_{33}$. Equation (37) into Eq. (38) gives

$$\Phi\left(1 + 5\varepsilon - \frac{1}{6}\frac{\gamma_1-\gamma_2}{\eta_c}\frac{\kappa_0}{K_{33}}\right) - \frac{V\mathrm{d}}{16}\frac{\gamma_1-\gamma_2}{K_{33}} = 0 \tag{40}$$

Eq. (39) into Eq. (40) gives

$$\Phi^3 + \frac{x_1}{x_2}\Phi - \frac{x_3}{x_2} = 0 \tag{41}$$

from which we get the expressions

$$\left.\begin{aligned} \Phi^2 &= \left(\frac{x_3}{x_1}\right)^2 - 2\frac{x_2x_3^4}{x_1^5} \\ \Phi^4 &= \left(\frac{x_3}{x_1}\right)^4 \\ \varepsilon &= x_4 + \frac{x_2}{5}\left(\frac{x_3}{x_1}\right)^2 - \frac{2}{5}\frac{x_2^2x_3^4}{x_1^5} \end{aligned}\right\} \tag{42}$$

to be inserted into Eq. (32) for the shear induced birefringence. We have used the abbreviations

$$\left.\begin{aligned} x_1 &= 1 + \frac{1}{2}\frac{\kappa_0}{K_{33}}\left(5 + \frac{1}{4}\frac{\gamma_1 - \gamma_2}{\eta_c}\right) \\ x_2 &= 5\left[1 + \frac{\kappa_0}{12K_{33}}\left(4 + \frac{\gamma_1 - \gamma_2}{\eta_c}\right) + \frac{\kappa_0^2}{576K_{33}^2}\left(4 + \frac{\gamma_1 - \gamma_2}{\eta_c}\right)^2\right]\frac{K}{3} \\ x_3 &= \frac{V\mathrm{d}}{16}\frac{\gamma_1 - \gamma_2}{K_{33}} \\ x_4 &= \frac{\kappa_0}{24K_{33}}\left(4 + \frac{\gamma_1 - \gamma_2}{\eta_c}\right) \end{aligned}\right\} \tag{43}$$

In the derivation of Eqs. (42) we have used $x_2\Phi^2/x_1 \ll 1$. If we insert the experimental values for the material parameters reported in Section V, it turns out that $x_2\Phi^2/x_1 < 10^{-2}$, so the approximations seem to be well justified in our case.

Finally, if we insert the expressions (42) into Eq. (32), and also use Eq. (33) we arrive, after some algebra, at

$$\frac{m}{\mathrm{d}} = a_2(V\mathrm{d})^2 + a_4(V\mathrm{d})^4 \tag{44}$$

where

$$a_2 = \frac{n_\perp}{\lambda_0}\left(1 - \frac{n_\perp^2}{n_\parallel^2}\right)\frac{4}{15}\left(\frac{\gamma_1 - \gamma_2}{16K_{33}}\right)^2\left[1 + \frac{2}{7}\frac{\kappa_0}{24K_{33}}\left(4 + \frac{\gamma_1 - \gamma_2}{\eta_c}\right)\right] \times \left[1 + \frac{1}{6}\frac{\kappa_0}{K_{33}}\left(5 + \frac{1}{4}\frac{\gamma_1 - \gamma_2}{\eta_c}\right)\right]^{-2} \tag{45}$$

and

$$a_4 = -\frac{n_\perp}{\lambda_0}\left(1 - \frac{n_\perp^2}{n_\parallel^2}\right)\frac{16}{315}\left(\frac{\gamma_1 - \gamma_2}{16K_{33}}\right)^4\left[17K[1 + U_1(\kappa_0)] + \tfrac{4}{3}[1 + U_2(\kappa_0)]\right] + \frac{1}{6}\frac{\kappa_0}{K_{33}}\left(5 + \frac{1}{4}\frac{\gamma_1 - \gamma_2}{\eta_c}\right)\Bigg]^{-5} \tag{46}$$

The functions $U_1(\kappa_0)$ and $U_2(\kappa_0)$ in Eq. (46) are polynomials with the properties $U_1(0) = U_2(0) = 0$. Since they are rather lengthy, and will not affect the evaluation of parameters, we do not write them down.

Summarizing this section, we have arrived at a solution of the shear flow problem valid for small velocities and weak electric fields. The tilt angle

$\phi(\zeta)$ and the velocity $u(\zeta)$ can be obtained from Eqs. (31) and (36), given the applied shear and electric field and the relevant elastic and viscous coefficients. The effective birefringence, which is the experimentally observed quantity, is then given by Eq. (44) together with Eq. (33). The method used in Section III is actually the reverse: Observing the change in birefringence of the liquid crystal layer caused by known shear rates and electric fields, the material parameter combinations occurring in Eqs. (45) and (46) can be determined.

III TORSIONAL SHEAR FLOW EXPERIMENT

a Experimental details

The compound used was 5CB (4-cyano-4'-pentyl-biphenyl), purchased from BDH, England, and used without further purification. The nematic range is 22.0–35.1°C.

The nematic layer is held between two circular glass plates (diameter 50 mm). The layer thickness can be varied using three micrometers, and the parallellity of the plates is checked optically by observing interference fringes in the empty cell. The lower plate is rotated by a synchronous ten-step gear motor. Along the axis of rotation an expanded He–Ne laser beam (wavelength $\lambda_0 = 632.8$ nm) is incident on the liquid crystal layer from below. The cell is mounted between crossed polarizers, and optical patterns in the sheared liquid crystal layer are viewed from above (cf. Figure 5).

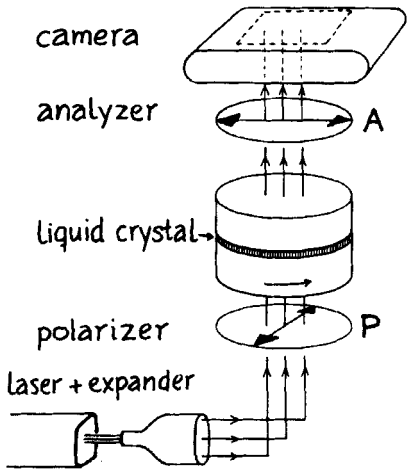

FIGURE 4 Schematic picture of the torsional shear flow apparatus. The laser light beam is expanded and enters the temperature chamber, where the liquid crystal flow cell is situated. The interference patterns seen in the flowing liquid crystal are recorded on a photographic film. P = polarizer and A = analyzer.

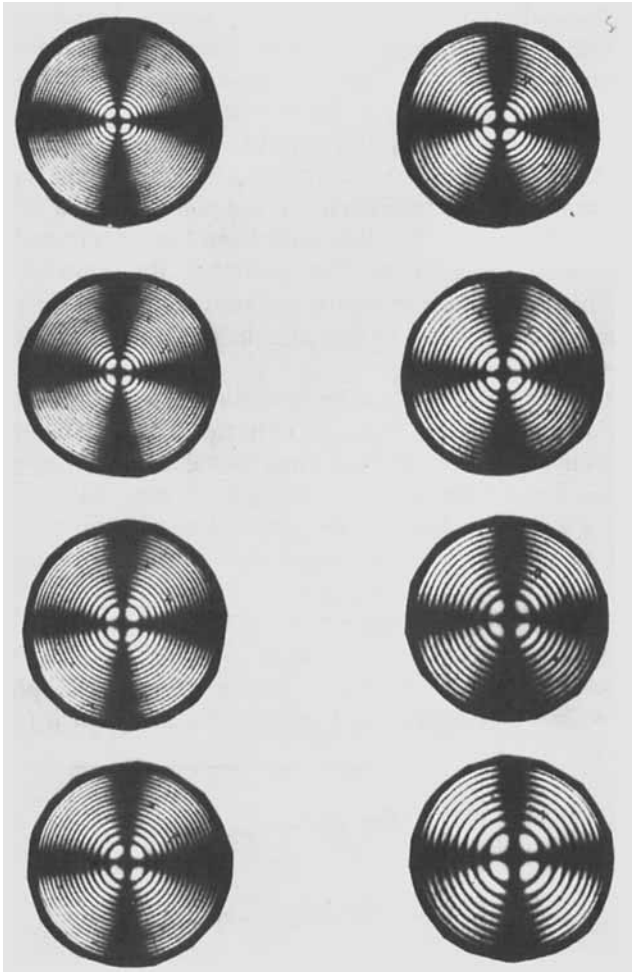

FIGURE 5 Some examples of interference patterns. The left row is at temperature $T = 23.1°C$ and the right at $T = 32.2°C$. All photographs shown were taken with an angular velocity for the lower plate $\omega = 10.9083 \times 10^{-5}\ s^{-1}$, and with a liquid crystal layer thickness $d = 300\ \mu m$. The difference within the rows is the applied voltage, being from top to bottom $U = 0$, 0.24, 0.42 and 0.55 V. It is seen that the rings move outwards when the field is applied, displaying the effect that the field decreases the mean value of the director angle ϕ across the layer, thereby diminishing the shear induced effective birefringence.

The experimental set-up is shown schematically in Figure 4. The whole apparatus is enclosed in a large temperature chamber with a hot air supply. The temperature of the chamber is controlled by a contact thermometer, and the temperature of the liquid crystal layer is measured with a thermistor probe near the glass plates. A temperature control of the liquid crystal to within 0.2°C is achieved in this way.

The nematic soaks into the cell by capillary actions. To admit the application of an electric a.c. field across the layer, the two glass plates have their inner surfaces coated with a very thin conducting film of tin oxide. The desired boundary conditions for the director (normal to the plates) are achieved by applying a thin layer of lecithin on the glass surfaces. When the lower plate is non-rotating, we thus have a nematic "single-crystal" with the director everywhere perpendicular to the plates. Viewed from above in the parallel laser light, the cell is dark (extinction between crossed polarizers). The interference patterns in the flow condition are recorded directly on a photographic film, using a Pentax 6 × 7 mirror reflex camera-housing. A measuring microscope is used to evaluate the photographs, of which a total of 180 were taken.

Looking back at Eq. (44), it can be viewed upon as a series expansion for the effective birefringence $\langle n_e - n_o \rangle / \lambda_0$ in terms of the combination Vd, the electric field dependence being contained in the constants a_2 and a_4. We choose thicknesses of the liquid crystal cell (d) and velocities ($V = \omega R$, where ω is the angular velocity of the lower plate relative to the upper one and R is the radius where we find a dark ring with ring number m) so that Vd is smaller than approximately 3×10^{-10} m^2 s^{-1}. Below this limit we find that a plot of $m/d(Vd)^2$ against $(Vd)^2$ shows a straight line for each value of the electric field. We have used $d = 200$, 300 and 500 μm, and $\omega = 4.36$, 10.91 and 21.82×10^{-5} s^{-1}. An example of such a plot (for temperature $T = 26.4$°C) is shown in Figure 6. We easily get $a_2(U)$ from the

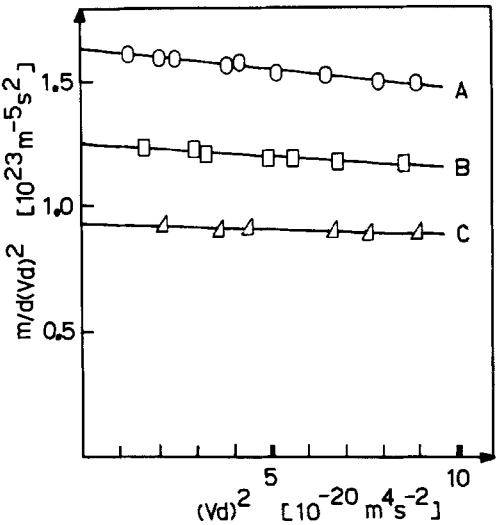

FIGURE 6 $m/d(Vd)^2$ as a function of $(Vd)^2$ for three different values of the applied electric field: A 0 V, B 0.34 V, C 0.49 V. ($d = 300$ μm, $T = 26.4$°C).

intercepts with the y-axis, and $a_4(U)$ from the slopes of the straight lines, fitted by the least squares method to the experimental points. The applied sine-wave voltage U (frequency 300 Hz) must be chosen so that the parameter ε in the ansatz Eq. (31) is always a small quantity. In the present experiments we have used $U = 0$, 0.24, 0.34, 0.42, 0.49 and 0.55 V.

b Evaluation of the experimental results

Which elastic and viscous constants can we get from the experimentally determined parameters $a_2(U)$ and $a_4(0)$? From $a_2(U)$ we could in principle get $(\gamma_1 - \gamma_2)/K_{33}$, $1/K_{33}$ and $(\gamma_1 - \gamma_2)/\eta_c$ by fitting the function Eq. (45) to the experimental points, knowing $n_\parallel$, $n_\perp$ and ε_a. However, it turns out that $a_2(U)$ is only weakly dependent on the term $(\gamma_1 - \gamma_2)/\eta_c$, originating from the second term in Eq. (37), so that all three parameter combinations cannot be determined in practice, mainly because we are restricted to use weak electric fields (small values on κ_0) in order to keep the parameter ε in Eq. (31) small. On the other hand, we cannot leave out the term $(\gamma_1 - \gamma_2)/\eta_c$ in $a_2(U)$ because of its magnitude compared to the other terms. Roughly speaking, the term comes in too weakly to be accurately determined, but too strongly to be neglected. The course we have taken to overcome this difficulty is to determine the Miesowicz viscosity η_c in a separate experiment, described in Section IV. Knowing η_c, we easily get values for $(\gamma_1 - \gamma_2)/K_{33}$ and $1/K_{33}$ from a fit of $a_2(U)$. Those plots are shown in Figure 7 for all the five temperatures used in the experiment. From the slopes $a_4(0)$ we get $K = (K_{33} - K_{11})/K_{33}$. From our earlier determination of the ratio γ_1/γ_2 (Ref. 12) we can then separately obtain γ_1 and γ_2. The values used for the refractive indices $n_\parallel$ and $n_\perp$, and for the dielectric anisotropy ε_a were taken from Karat and Madhusudana[10] and Dunmur,[11] respectively. They are reproduced in Table I.

Summarizing, we get as results from the torsional shear flow experiment $K_{11}(T)$, $K_{33}(T)$, $\alpha_2(T)$ and $\alpha_3(T)$ (the latter two through the relations $\gamma_1 = \alpha_3 - \alpha_2$ and $\gamma_2 = \alpha_3 + \alpha_2$), if we can supply $\eta_c(T)$ from a separate determination, which is the aim of the Poiseuille flow experiment.

TABLE I

Refractive indices and dielectric anisotropy for 5CB

T_{XN} (°C)	T_{NI} (°C)	T (°C)	$n_\parallel$	$n_\perp$	ε_a
22.0	35.1	23.1	1.713	1.529	11.5
		26.4	1.703	1.530	10.9
		29.7	1.693	1.532	9.8
		32.2	1.682	1.536	8.5
		34.1	1.669	1.542	6.6

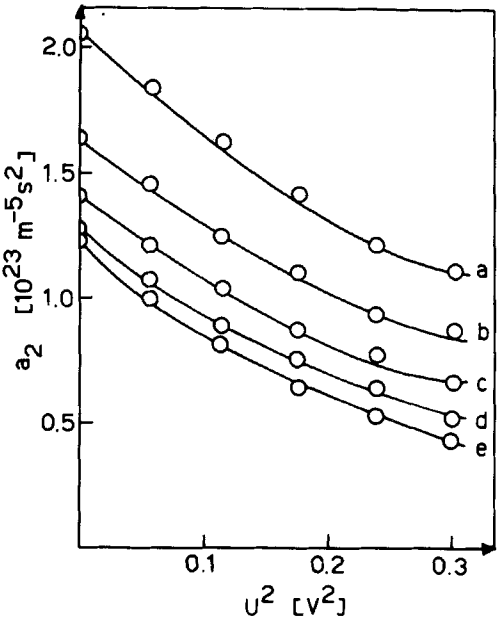

FIGURE 7 a_2 as a function of the applied voltage squared, U^2. The points in this figure contain the information from all the photographs taken in the torsional shear experiment. The letters to the right stand for different temperatures: (a) 23.1, (b) 26.4, (c) 29.7, (d) 32.2 and (e) 34.1°C. A fit of a_2 to the experimental points according to Eq. (45) will yield values for the material parameters for the liquid crystal as discussed in Sec. IIIb.

IV POISEUILLE FLOW EXPERIMENT

The Miesowicz viscosity η_c, one of the three principal "locked director viscosities" for nematics, is the viscosity measured with the director along the velocity gradient in a flow experiment.[13] To measure η_c we have made a capillary viscometer, where the liquid crystal is driven through a rectangular capillary by a known, constant pressure difference.

The capillary had dimensions 50 × 3.9 × 0.25 mm. A schematic picture of the set-up is shown in Figure 8. The constant pressure difference between the ends of the capillary was supplied by two large pressure-vessels, with a slight pressure difference generated by two rubber balls. Because of the large volume of the pressure-vessels compared to the volume changes occurring during the experiment when the nematic is flowing through the capillary, the pressure difference is very nearly constant. To measure the viscosity, the time is taken for a certain volume of the liquid crystal (measured on the scales of the graduated tubes) to pass the capillary under a known

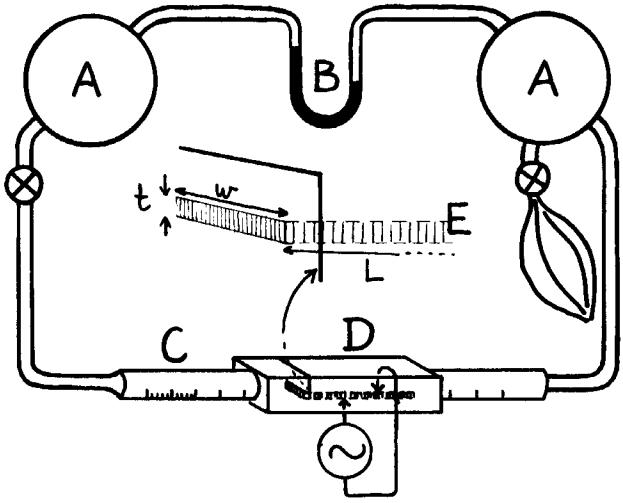

FIGURE 8 A schematic picture of the Poiseuille flow set-up. A pressure-vessels, B water manometer, C graduated tubes, D flow cell, E liquid crystal flowing in the graduated tubes and through the flow cell. Shown also is the generator used for the application of an electric a.c. field across the rectangular flow capillary.

pressure difference. The viscosity could then in principle be found from the standard formula[14]

$$\eta = \frac{Pwt^3}{12LQ}$$

where t is the capillary thickness, w the width and L the length. P is the pressure difference driving the flow, and Q is the flow rate (volume/time).

However, because of the large errors that may arise, especially from the uncertainty in thickness t, which appears in the formula to the third power, this method was not used. Instead, sucrose solutions of different concentrations were used to calibrate the viscometer.[15] The viscosities of the calibration solutions were determined in a standard Ubbelohde viscometer.[16]

The upper and lower glass plates have their inside coated with a thin conductive layer (SnO_2), permitting the application of an electric a.c. field across the sample (frequency $f = 300$ Hz). The field will lock the director along the velocity gradient (perpendicular to the plates) since $\varepsilon_a > 0$ for 5CB. With no field applied and at sufficiently high flow rate we are in the flow alignment region: Except at two boundary layers at the surfaces and one layer in the center, the director can be considered to make an angle θ_0 to the flow direction (the flow alignment angle), which is of constant magnitude throughout the cross-section. Distortions in form of disclinations

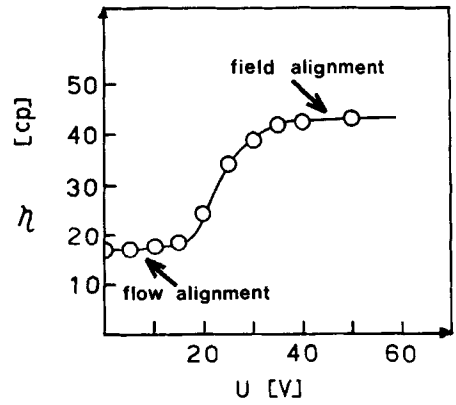

FIGURE 9 Effective viscosity as a function of applied voltage U. Below about 15 V the flow dominates the influence of the field, and the director makes a small angle θ_0 to the velocity. Between 15 and 40 V we have a transition region where the director is a complicated function of applied field and velocity. Above 40 V the situation simplifies again, the director being locked by the field in a direction perpendicular to the velocity (along the field). It is in this situation we measure the Miesowicz viscosity η_c.

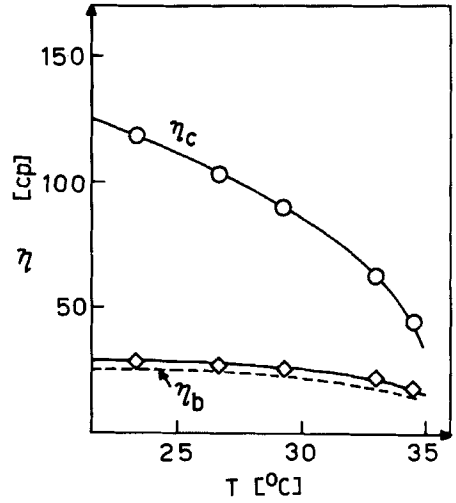

FIGURE 10 Measured Miesowicz viscosity η_c as a function of temperature T. Also shown is the effective viscosity $\eta \gtrsim \eta_b$ measured in the flow alignment region in Figure 9. Dotted line corresponds to η_b estimated from the expression $\eta = \eta_b \cos^2\theta_0 + \eta_c \sin^2\theta_0$ with θ_0 values taken from Ref. 12.

and walls can be seen in a microscope between crossed polarizers. With a sufficiently strong field applied, however, the director was observed to be uniform in the sample during the flow. This is the situation in which the viscosity η_c was measured. It corresponds to the part named field alignment in Figure 9, where the viscosity is shown as a function of applied field at the temperature $T = 34.5°C$. It is seen that for voltages above approximately 40 V the viscosity tends to a constant value $\eta_c = 44$ cp. For these voltages the electric field is strong enough to dominate the influence of the viscous torques on the director, and consequently the director will align uniformly perpendicular to the plates. In the part of Figure 9 named flow alignment, due to the small value of the alignment angle θ_0, the measured viscosity is nearly equal to the Miesowicz viscosity η_b.

The same temperature chamber was used as in the torsional shear flow experiment. The measured Miesowicz viscosities as a function of temperature for 5CB are shown in Figure 10. All measurements of η_c were made with an applied voltage $U = 50$ V.

V RESULTS AND DISCUSSION

We now get the elastic and viscous constants $K_{ii}(T)$ and $\alpha_i(T)$ by the procedure described at the end of Section III. The results are shown in Figures 11 and 12. In Figure 11 is also shown the ratio K_{11}/K_{33}, which is found to be nearly constant in the nematic range. The value for the twist viscosity γ_1 as a function of temperature is shown in Figure 13 together with γ_2 and the ratio γ_1/γ_2, which determines the director alignment in a local shear.

The elastic constants K_{11} and K_{33} for 5CB have been measured by Karat and Madhusudana[10] using the Fredericksz-transition technique. The values for the elastic constants found in those experiments are about 50–100% higher compared to our values in Figure 11. It has been pointed out to us that the values of Ref. 10 were calculated using estimates of χ_a which turn out to be too high by about a factor of two. With new values for the susceptibility anisotropy the elastic constants measured by Karat and Madhusudana seem to be comparable to ours. The elastic constants have also been determined by Maze,[17] analyzing the capacitance-voltage curve in a nematic sample, and values between ours and those of Ref. 10 are obtained. We do not intend to take up here the discussion of Ref. 10 on the validity of the mean-field theory for 5CB, but merely note that we find the ratio K_{11}/K_{33} to be constant within the experimental errors in the nematic range, as predicted by mean-field theory,[18] while in Ref. 10 this ratio is found to increase with temperature.

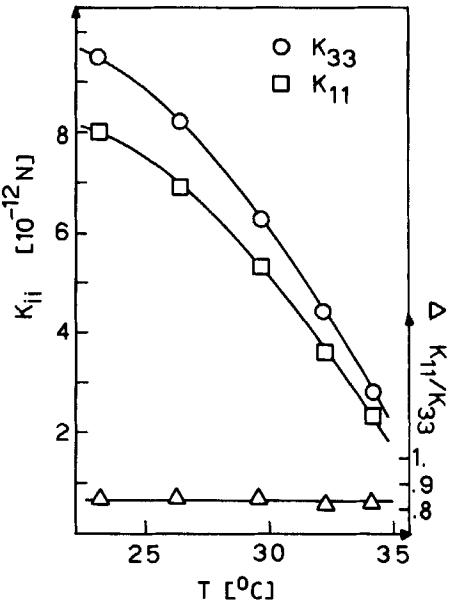

FIGURE 11 Experimental results for the elastic constants K_{11} and K_{33} as a function of temperature T. Shown also is the ratio K_{11}/K_{33} (scale to the right).

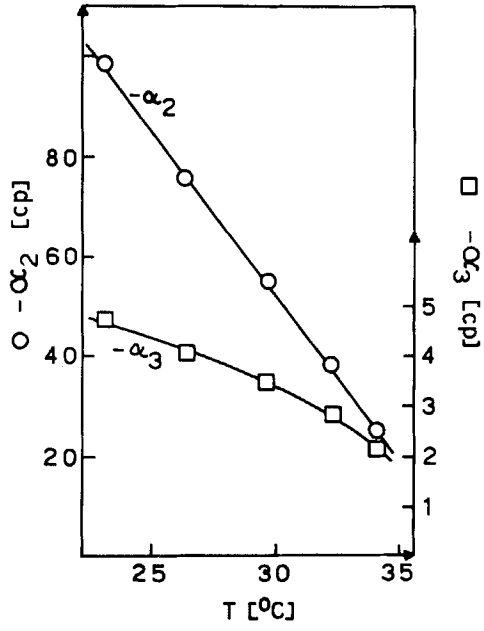

FIGURE 12 Experimental results for the viscosities α_2 and α_3. Scale to the left for α_2 (upper curve) and to the right for α_3 (lower curve). Note: Negative values.

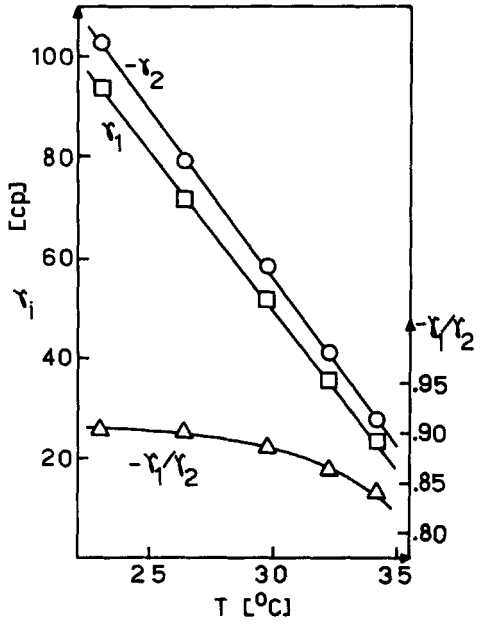

FIGURE 13 The viscosities $\gamma_1 = \alpha_3 - \alpha_2$ and $\gamma_2 = \alpha_3 + \alpha_2$ and their ratio γ_1/γ_2 as a function of temperature T.

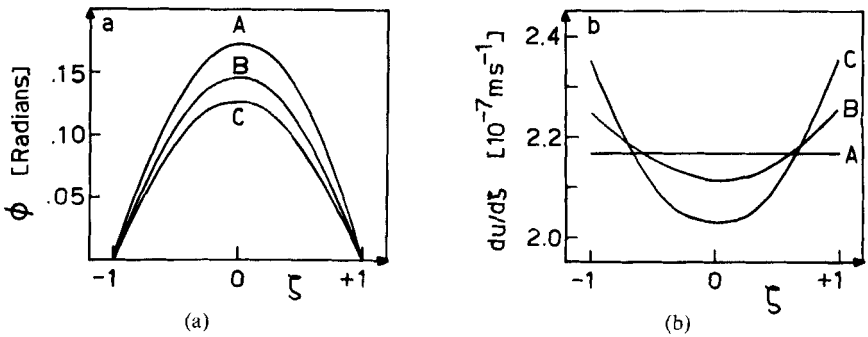

FIGURE 14 Tilt angle ϕ (a) and velocity gradient $du/d\zeta$ (b) as a function of reduced coordinate ζ for three different applied voltages: A 0 V, B 0.34 V and C 0.55 V. $T = 23.1°C$, $V = 4.36 \times 10^{-7}$ ms^{-1} and $d = 300$ μm.

Finally, with our experimentally determined parameters, we can calculate the director profile through the sample according to our ansatz Eq. (31), and then from Eqs. (35) and (37) the corresponding velocity profile. In Figure 14 such profiles are shown for the temperature $T = 23.1°C$ at different applied electric fields. Looking at this figure we see that, even if the director tilt is changing markedly through the sample (A), as is always the

case at low shears, the shear (velocity gradients) is itself practically constant in the absence of an electric field. The applied field (B, C) has the effect of lowering the shear in the middle and increasing it near the boundaries. This is a combined effect of the strong anchoring boundary condition and the effect of the field on the apparent viscosity: the field increases the viscosity and decreases the velocity gradient in the middle of the sample, leaving for the outer regions to compensate for the finite velocity difference between the plates.

Acknowledgements

This research was sponsored by the Swedish Science Research Council (Contracts 3361–010/014) and by the Swedish National Board for Technical Development (Contract 76–4277).

Note

After the completion of our manuscript we have noticed the recent article by J. Wahl, *Z. Naturforsch.* **34a**, 818 (1979). Wahl discusses shear flow in the presence of an electric field for MBBA which is a material with negative dielectric anisotropy. This means that the field itself has a similar effect as the shear, instead of counteracting it as in our case. Wahl's analysis is considerably different from ours. In particular he makes the simplification that the electric field has no influence on the velocity gradient, which might be valid in his case of MBBA, where the dielectric anisotropy is about a tenth of that for 5CB.

References

1. For a review see, for example, J. T. Jenkins, *Ann. Rev. Fluid. Mech.*, **10**, 197 (1978).
2. O. Parodi, *J. Physique*, **31**, 581 (1970).
3. J. Wahl and F. Fischer, *Mol. Cryst. Liq. Cryst.*, **22**, 359 (1973).
4. Th. Walterman and F. Fischer, *Z. Naturforsch*, **30a**, 519 (1975).
5. S. Holmström and S. T. Lagerwall, *Mol. Cryst. Liq. Cryst.*, **38**, 141 (1977).
6. F. M. Leslie, *Arch. Ratl. Mech. Anal.*, **28**, 265 (1968).
7. S. Chandrasekhar, *Liquid Crystals* (Cambridge, 1977), p. 106.
8. P. G. de Gennes, *The Physics of Liquid Crystals* (Oxford, 1974), p. 171.
9. M. J. Stephen and J. P. Straley, *Rev. Mod. Phys.*, **46**, 617 (1974).
10. P. P. Karat and N. V. Madhusudana, *Mol. Cryst. Liq. Cryst.*, **36**, 51 (1976).
11. D. A. Dunmur, Private communication.
12. K. Skarp, S. T. Lagerwall, B. Stebler and D. McQueen, *Physica Scripta*, **19**, 339 (1979).
13. M. Miesowicz, *Bull. Int. Akad. Polon. Sci. Lett. Ser. A*, **28**, 228 (1936).
14. M. G. Kim, S. Park, Sr., M. Cooper, and S. V. Letcher, *Mol. Cryst. Liq. Cryst.*, **36**, 143 (1976).
15. Iscotables (ISCO Corp. USA), Fifth Ed., p. 15 (1974).
16. J. R. Van Wazer, J. W. Lyons, K. Y. Kim and R. E. Colwell, *Viscosity and Flow Measurement* (Interscience Publishers, New York, 1963), p. 224.
17. C. Maze, *Mol. Cryst. Liq. Cryst.*, **48**, 273 (1978).
18. A. Saupe, *Z. Naturforsch*, **15a**, 810 (1960).
19. P. Pieranski and E. Guyon, *Phys. Rev.*, **A9**, 404 (1974).